_____

Unterschrift Betreuer

TECHNISCHE
UNIVERSITÄT
WIEN
Vienna University of Technology

DIPLOMARBEIT

Reorganizing the Cortical Actin Skeleton using Micropatterning

ausgeführt am Institut für Angewandte Physik

der Technischen Universität Wien

unter der Anleitung von

Prof. Dr. Gerhard Schütz

und

Dr. Eva Sevcsik

durch

Angela Koffler

Oktober 2017

_____

Unterschrift Student

Contents

Abstract

The mammalian plasma membrane is a fluid and highly functional semi-permeable barrier between the cell and its environment. It consists of proteins and lipids which are not homogeneously distributed, but show local and temporal heterogeneity. Different mechanisms are suspected to be responsible for membrane heterogeneity, such as lipid-lipid and lipid-protein interactions. In addition, the cortical actin cytoskeleton has been proposed to restrict the motion of proteins and even form diffusion barriers to lipids. Such corrals created by actin are thought to be very small – around 100 nm – making them hard to address experimentally.

The aim of this work was to establish a method capable of testing the role of actin in the diffusion behavior of lipids and membrane proteins. For this, a protein micropatterning approach to reorganize the cortical actin skeleton of live cells was used, allowing the measurement of protein and lipid mobility as a function of the local actin density.

Zusammenfassung

Die Plasmamembran von Säugetierzellen ist eine fluide und hoch gradig funktionale semipermeable Barriere zwischen der Zelle und ihrer Umgebung. Sie besteht aus Proteinen und Lipiden, die nicht homogen verteilt sind, sondern lokale und zeitliche Heterogenitäten aufweisen. Von verschiedenen Mechanismen, unter anderem Lipid-Lipid und Lipid-Protein Wechselwirkungen, wird vermutet, dass sie verantwortlich für diese Heterogenitäten in der Membran sind. Weiters kann das kortikale Aktin-Zytoskelett die Beweglichkeit von Proteinen einschränken und sogar Diffusionsbarrieren für Lipide formen. Es wird vermutet, dass diese durch Aktin entstandene Korräle sehr klein – um 100 nm – sind, was sie experimentell schwer zugänglich macht.

Das Ziel dieser Arbeit war es, eine Methode zu entwickeln, die es möglich macht, die Rolle, die Aktin im Diffusionsverhalten von Lipiden und Membranproteinen spielt, zu untersuchen. Wir haben Methoden der Mikrostrukturierung verwendet um das kortikale Aktinskelett lebender Zellen umzuorganisieren. Dies sollte es ermöglichen, die Mobilität von Proteinen und Lipiden als Funktion der Aktindichte zu messen.

1 Introduction

1.1 Motivation

The plasma membrane of cells serves as a barrier between the inside and outside of the cell. The membrane consists of a lipid bilayer, which is stable due to hydrophobic interactions of the lipid tails. It is thus nearly impossible for charged or polar molecules to pass through the hydrophobic core of the plasma membrane. To enable the cell to nevertheless sense, exchange with, and move in its surroundings, a multitude of different proteins are embedded in and attached to the plasma membrane that provide channels and participate in signaling processes.

The plasma membrane consists of thousands of different proteins and lipids, with proteins accounting for approximately half of its mass. The spatial distribution of those molecules in as well as across the membrane plane is heterogeneous. Some types of lipids and proteins can only be found in the cytosolic, some only in the extracellular leaflet of the plasma membrane, and transmembrane proteins have a typical orientation across the membrane.

Laterally, proteins and lipids are distributed inhomogeneously, too. It is believed that local and temporal inhomogeneities are necessary for the cell to perform functions such as receptor-mediated signaling, exo- and endocytosis, and cell movement. Different models have been developed to describe the organization of the plasma membrane, including theories about lipid domains as well as charge- and size-based interactions between lipids and proteins [1]. Actin has also been suggested to play an active part in domain formation and to hinder diffusion of protein and lipids [2].

In this work, the focus was on the role actin plays in organizing the plasma membrane. Cortical actin is a layer of proteins close to the inner side of the plasma membrane giving the cell its shape and stability. It is rich in actin filaments, which are, in various ways, anchored to the plasma membrane. Studies suggest that the cortical actin network does not only restrict the diffusion of membrane proteins directly anchored to it, but that the actin filaments themselves, as well as the anchored proteins, can serve as a barrier to otherwise freely diffusing proteins and lipids [3, 4]. The model put forward in these

studies is called the *membrane picket fence model*. The model suggests that molecules can diffuse freely in areas between the actin fences, but pass the fences only occasionally. This diffusion behavior has been termed *hop diffusion* and can only be observed with high time resolutions of approximately 25 µs or higher [5]. To date, this time resolution has only been achieved by single-particle tracking of proteins and lipids labeled with gold particles of 10 nm diameter, making influences of the label rather likely.

Our aim was to devise an alternative approach independent of directly observing hop diffusion to study the influences of actin on the diffusion of lipids and proteins. The idea was to reorganize the cortical actin in living cells into actin-enriched, µm-sized areas, enabling us to measure the diffusion behavior of proteins in dependence of cortical actin density within a single cell. This would allow to identify proteins and/or lipids that were affected in their distribution and mobility by cortical actin.

Reorganization of the cortical actin was realized by a technique called *protein micropatterning*. In this technique, stamps are used to print proteins onto a glass surface in µm-sized patterns, and cells are interfaced with these structures. Here, cells expressing a transmembrane protein chimera that binds to the proteins of the pattern on the glass and to the cortical actin on the inner side of the cell were used. This way, we hypothesized, the transmembrane protein should arrange the cortical actin congruently with the stamped protein pattern.

Furthermore, to optimize the micropatterning protocol, the methods already established in our laboratory were compared with the method used in the group of Jacob Piehler [6].

1.2   The Actin Cytoskeleton

The cytoskeleton consist mainly of three different filament types: *Intermediate filaments* are responsible for mechanical stiffness, *microtubuli* define the position of membrane-encapsulated organelles and are used for intracellular transport, and *actin* is responsible for the shape of the plasma membrane and movement of the entire cell.

Actin, like all cytoskeleton filaments, consists of small proteins. Its fibers are highly dynamic and can assemble and disassemble quickly. The filaments of actin are polarized,
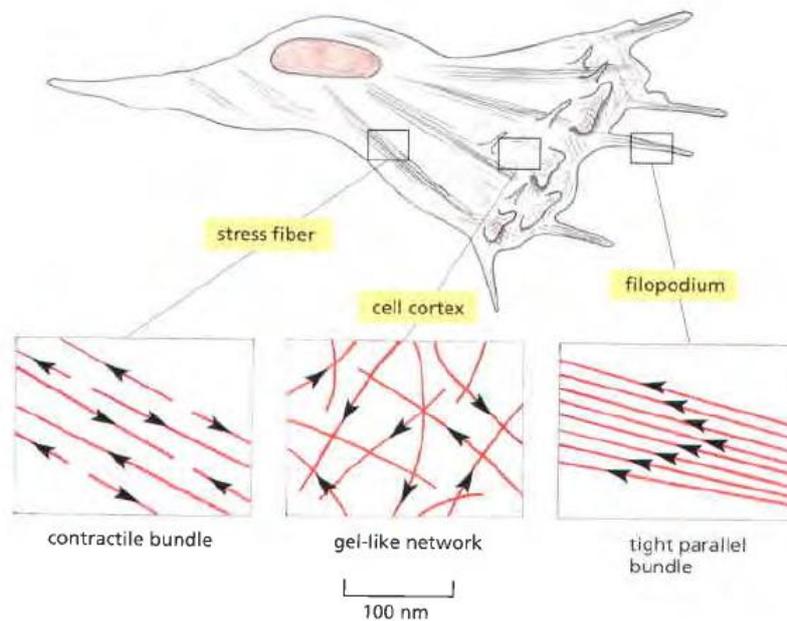
Figure 1: Actin Filaments in the Cell
Illustration of a fibroblast in a culture dish. Actin filaments are shown in red, the arrows point toward their minus-ends [7].

the *plus-end* being fast-growing and *minus-end* slow-growing. Figure 1 shows typical actin filament assemblies in fibroblasts.

Actin filaments can self-assemble into different structures: *Actin cables* are long bundles of parallel actin filaments that can be found in stress fibers and filoepodia. *Actin patches* are gel-like networks of actin fibers, and are associated with the cell cortex, which is why they are also called *cortical actin* [7].

Proteins of the ERM-family (named after the first member proteins discovered: Ezrin, Radixin and Moesin) serve as linkers between the plasma membrane and the cortical actin network by binding to actin and to the cytosolic part of transmembrane proteins.

In this work, the actin-binding domain of Ezrin was part of a constructed transmembrane protein chimera designed to reorganize the cortical actin according to a pattern imposed from the outside of the cell.

1.3   Organization of the Plasma Membrane

1.3.1   Components of the Plasma Membrane

The plasma membrane separates a biological cell from its environment. The membrane is formed by lipids, which self-assemble into a fluid-like bilayer. A variety of proteins are embedded in (integral proteins) or anchored to (peripheral proteins) the plasma membrane, fulfilling different functions, such as transport of molecules through the plasma membrane, communication with and sensing of the cell's surroundings, and movement of the cell through its environment. Most of the plasma membrane's components can move along the membrane. Studying their movement behavior can give clues about the size of the lipid or protein, its interaction with other molecules, or its function in signaling cascades [7].

1.3.2   Measuring Diffusion Using Single Molecule Tracking

To visualize the movement of a certain type of lipid or protein in the plasma membrane through microscopy, it has to be labeled with a fluorophore, which has to be excited by a powerful light source (laser), and the emitted light has to be captured by a sensitive camera (e.g. CCD camera), all while keeping the background signal low (e.g. with TIRF, see Section 1.5). A computer algorithm is used to find the positions of the fluorescent signals in the captured images, and to trace their movement across subsequent images. From this information, trajectories of individual fluorophores can be reconstructed. Those reconstructions are the foundation of *single molecule tracking*.

1.3.3   Mean Square Displacement

Features often used to describe diffusion behavior are the mean square displacement (MSD) $\langle r^2 \rangle = [\vec{r}(t_0) - \vec{r}(t_0 + \Delta t)]^2$, as a function of time t, and the diffusion coefficient D, which has the dimension $\frac{\mathrm{m}^2}{\mathrm{s}}$.

A commonly-used method to represent different movement types is to plot the mean square displacements (MSD(Δt) or $\langle r^2 \rangle (\Delta t)$) as a function of Δt.

The diffusion distance $(\vec{r}(t_n) - \vec{r}(t_n + \Delta t))$ used in calculating the MSD is the difference in location of one particular particle at times t_n and $t_n + \Delta t$, not regarding the path it may have taken in the meantime. For one trajectory, the MSD would be calculated in the following way:

$$\text{MSD}(\Delta t) = \frac{\sum_{n=1}^{N}[\vec{r}(t_n) - \vec{r}(t_n + \Delta t)]^2}{N}$$

.

Here, Δt has to be a multiple of the inverse frame rate $\frac{1}{\tau_f}$ the trajectory was recorded with. N is the number of usable distances, which can be calculated, given the number N_{total} of frames this trajectory is measured over, via $N = N_{\text{total}} - \Delta t \cdot \tau_f + 1$ [8]. In Figure 2, MSD plots of particles with different diffusion characteristics are shown. Their differentiation into diffusion categories is described in the following.

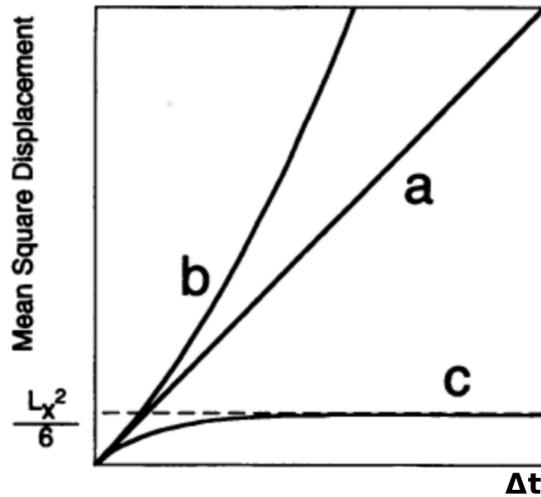**Figure 2: MSD Plots for Different Diffusion Types**
Theoretical MSD plots are shown for different diffusion types in one dimension with the same short-term diffusion constant D. Δt is plotted along the abscissa and the MSD as a function of Δt along the ordinate.
a: Brownian diffusion
b: directed diffusion
c: confined diffusion in a confinement between 0 and L_x
Image adapted from [4].

9

1.3.4   Diffusion Categories

MSD plots and the diffusion constant can be used to classify the movement of a molecule into different categories:
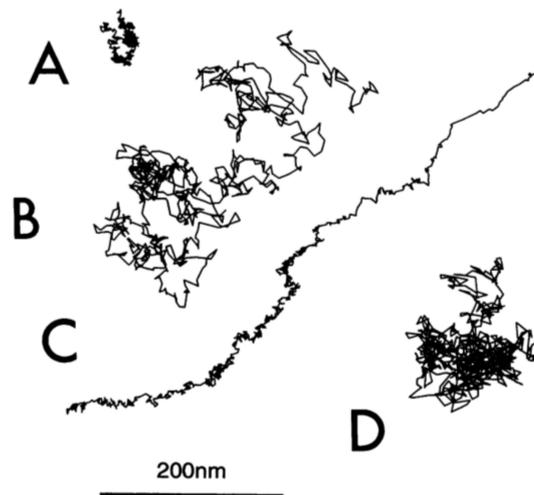
Figure 3: Typical Trajectories of Plasma Membrane Proteins
Kusumi et al. [4] distinguish between different diffusion types for gold particles attached to E-cadherin:
A: stationary mode
B: Brownian (or free) diffusion
C: directed diffusion
D: confined (or restricted) diffusion
Image adapted from [4].

Trajectory **A** in Figure 3 shows a particle in stationary mode (Kusumi et al. define every trajectory with a diffusion constant of $4.6 \cdot 10^{-12} \frac{\mathrm{cm}^2}{\mathrm{s}}$ or less as stationary [4]). Small movements can still be observed in "non-moving" particles due to imaging imprecision, or, in case of fluorophores, due to their movement relative to the molecule they are attached to, even if the latter itself is immobile.

The trajectory in **B** is an example for Brownian (or free) diffusion. This diffusion type is purely random regarding the direction of the movement. On a two-dimensional surface, the Brownian diffusion behavior can be described with $\langle r^2 \rangle = 4Dt$, or $\langle r^2 \rangle = 4Dt + 4\sigma^2$ when including position measurement imprecision.

In contrast to Brownian motion, directed diffusion (**C**) has a preferred direction of movement. Directed diffusion movement can be described as a drift velocity v in one direction superimposed with Brownian diffusion, resulting in $\langle r^2 \rangle = 4Dt + v^2t^2$.

Trajectory **D** shows confined diffusion, which can be understood as Brownian diffusion inside a restricted area. Here, the mathematical description of the relation between diffusion constant and MSD is much more complex, since it also depends on the geometry of the confinement.

1.3.5   Hop Diffusion

Many studies compared the diffusion coefficients of proteins and lipids in artificial membranes and membrane blebs, in which the membrane skeleton is largely depleted, with those found in membranes of living cells (reviewed in [5]). Consistently, diffusion was found to be 5 to 50 times slower in live cell membranes. In the same review, Kusumi et al. showed that by looking at the diffusion of proteins and lipids in the membrane of living cells with a higher time resolution, the observed diffusion pattern can change from Brownian motion to a so-called *hop diffusion*. In this diffusion pattern, a particle moves similarly as in confined diffusion explained above, but also has the ability to escape its confinement area by hopping to an adjacent one (see Figure 4). Interestingly, the diffusion constant inside the confinement areas is similar to the diffusion constants obtained in artificial membranes and membrane blebs [5, 9]. This observation led to the formulation of the *membrane skeleton fence model*:

1.3.6   Membrane Skeleton Fence and Membrane Skeleton Picket Fence Model

The membrane skeleton fence model proposes an explanation for hop diffusion. It states that the cortical cytoskeleton serves as a barrier to diffusing proteins and lipids in the membrane, effectively forming the confinements observed in hop diffusion [10].

To also explain hop diffusion of lipids located at the outer layer of the cell membrane, which should not be influenced by the cortical membrane skeleton since the latter is located only at the inside of the plasma membrane, the *membrane skeleton picket fence model* has been suggested [9]. This model takes transmembrane proteins into account,
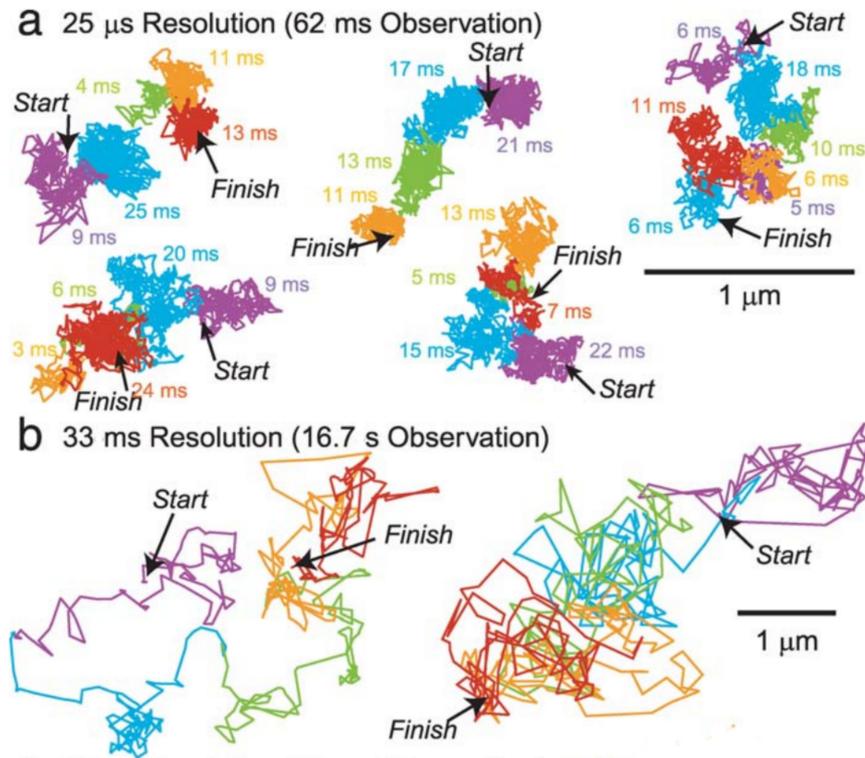
Figure 4: Hop Diffusion Observed with Different Time Resolutions

The trajectories shown are colloidal-gold-tagged lipids (L-α-dioleoylphosphatidylethanolamine)
diffusing in the plasma membrane of healthy rat kidney epithelial cells.

a: *Time resolution of 25* μs*, supposedly different compartments are colored in different colors.*

b: *Time resolution of 33* ms*; these trajectories were classified as Brownian motion, the colors in-*
dicate the passing of time.

This figure shows the importance of time resolution for diffusion behavior studies since hop diffu-
sion can be observed in a *but not in* b*, although the same lipid is observed.*

Image adapted from [5].

which bind to the cortical cytoskeleton at the inside of the cell, and so extend the diffu-
sion barrier through the membrane bilayer.

1.4   Micropatterning

Having this in mind, our goal was to manipulate the cells in a way that allowed us to influ-
ence the local concentration of cortical actin at will. This approach should provide a novel

experimental platform to measure the influence of local actin density on the diffusion of different proteins and lipids.

The experimental approach chosen to realize areas of defined actin densities within living cells was to involve microstructuring of the transmembrane protein chimera GFP-transmembrane-Ezrin (GFP-TM-Ezrin), designed to transmit the pattern imposed from the outside of the cell to the cortical actin. Monomeric green fluorescent protein (mGFP) constituted the extracellular domain of this protein and was used a) as an anchor to the patterned GFP antibody on the glass slide (referred to as "active coating" in the following) and b) as a fluorescent reporter on the local density of the patterned protein. The GFP was fused to a hydrophobic transmembrane helix (originated from the Fc receptor of IgG) residing in the plasma membrane (TM), followed by the actin-binding domain of Ezrin on the cytoplasmic side [11]. In order to be able to find causal relations between the diffusion behavior and the actin concentration, it is important to make sure that possible correlations are not due other reasons like a restriction of diffusion due to the anchored GFP-TM-Ezrin proteins themselves, or the decreased distance of the plasma membrane to the glass surface in the active patterned regions, which could hinder proteins with large extracellular domains to enter this regions at all. To control for this, an additional cell line expressing a protein of similar structure, but with a point mutation in the actin-binding domain of Ezrin (GFP-TM-Ezrin*) was made. This protein is not able to bind to actin anymore, but has the same potential to hinder diffusion by itself, making it possible to correct for influences to the diffusion behavior other than those caused by the patterned actin itself. Retroviral infection of target cells with the plasmids was used to create cells stably expressing these proteins.

The functionalized patterned surface was realized by micro-contact printing (see Section 2.2 for the protocol). Different substrates were transferred to the glass surface using PDMS stamps with various features in the micrometer range to create the active coating areas "A" (Figure 5). The partially coated surface was then backfilled with compounds that should passivate and/or promote cell adhesion, creating the background coating area "B". Next, active compounds were added that bound to the patterned substrate and the mGFP of the GFP-TM-Ezrin. Cells expressing GFP-TM-Ezrin were seeded onto those patterned glass surfaces, transmitting the pattern of the active coating to the actin skeleton (see Figure 6).
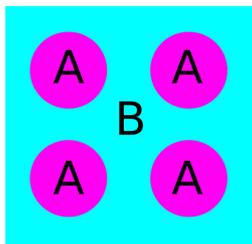
Figure 5: Illustration of a Micropatterned Surface

Illustration of a surface with micropatterned coating showing a possible pattern of active coated areas "A" and background coating "B".
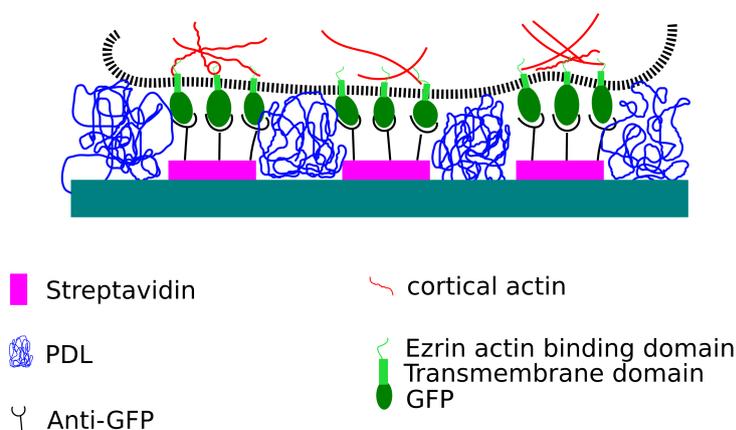
Figure 6: Actin-Patterned Cell

This cartoon shows how the cortical actin of a cell is patterned. Here, the active pattern is formed by streptavidin and a biotinylated antibody against GFP (anti-GFP). The background coating material is poly-D-lysin.

For the micropatterning protocols, either plasma-cleaned or epoxy-functionalized glass cover slips were used. By plasma-cleaning coverslips, OH groups are freed, which turns the surface into a highly hydrophilic one, onto which the compounds can adhere. The epoxy groups on the other hand can bind convalently to primary lysines in proteins.

1.4.1   Compounds Forming the Background Coating

The compounds used for the background coating area "B" were mainly chosen for their capacity to promote cell adhesion. In this work, different molecules were used for this purpose:

Fibronectin (FN) is a large glycoprotein that natively is part of the extracellular matrix. It binds to integrins (RGD binding proteins) and thereby to cell surfaces. One potential drawback of this particular background coating is its ability to cause actin polymerization [12], which could interfere with our experiments.

Poly-D-lysine (PDL) and poly-L-lysine (PLL) are synthetic positively charged polypeptides. They enhance the adhesion of the negatively charged cell surfaces by electrostatic attraction.

Bovine serum albumin (BSA) was used in the original protocol developed in our lab. It was used to passivate the epoxy surface. In our experiments, cells did not adhere onto BSA-coated surfaces.

PLL-PEG-RGD is PLL fused to a polyethylene glycol (PEG) and a RGD peptide. This compound binds to integrins similarly to FN.

1.4.2   Specific Binding Compounds Forming the Active Coating

The active coating area "A" consists of primary compounds used for printing, and secondary compounds that bind to both the primary compounds and the mGFP of GFP-TM-Ezrin and GFP-TM-Ezrin*.

Streptavidin is a protein which binds to biotin with high specificity and affinity. Thus, **biotinylated antibodies** can be easily attached to the patterns. Here, a biotinylated monoclonal GFP antibody was used to pattern GFP-TM-Ezrin.

PLL-PEG-HTL is a PLL fused to a PEG and a HaloTag ligand (HTL). The HTL binds specifically to the modified enzyme HaloTag (HT), so **HT-fused GFP-nanobodies** (HT-antiGFP) can be used to create an anti-GFP pattern.

1.5   Fluorescence

For a long time, low contrast used to be a big challenge in light microscopy. This changed radically with the use of fluorescent dyes.

Fluorophores have the ability to absorb and emit electromagnetic waves within a specific spectrum. The spectra of the green fluorescent protein (GFP) are shown in Figure 7. The emission spectrum is always shifted to the red relative to the absorption spectrum, since some energy is "lost" due to relaxation from the vibrational states to S1, as depicted in Figure 8; this effect is called Stokes Shift. Changing the wavelength of the excitation light only changes the probability of absorption, but not the shape of the emission spectrum.
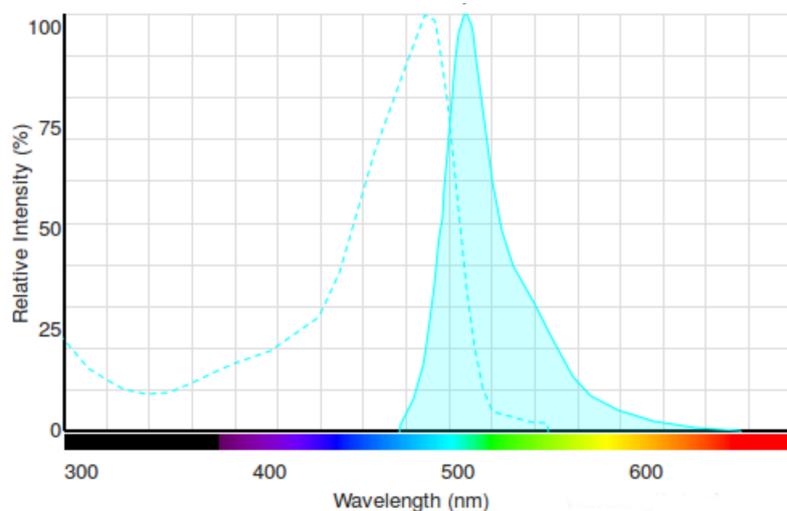

Figure 7: Emission and Absorption Spectra of GFP
The figure shows the absorption spectrum (dotted line) and the emission spectrum (solid line) of GFP. Image adapted from [13].

The underlying principle of fluorescence will be explained here using the Jablonski diagram in Figure 8. The energy of electromagnetic waves with wavelengths in the absorption spectrum lifts the fluorophore into an excited state within femtoseconds. From this state, it relaxes into its S1 state within picoseconds. Now the fluorophore can emit a photon in order to release energy and return to its ground state, or it can transfer into its triplet state (also called dark state). The process of absorption and subsequent fluorescent emission happens orders of magnitudes faster than the time resolution of the used cameras (milliseconds), leading to the impression of a constant light emission. Photoemission from the triplet state (phosphorescence) happens around ten orders of magnitude slower than photoemission directly from the S1 state. A fluorophore which is in its triplet state during acquisition time contributes fewer photons to the image than it would by transition-
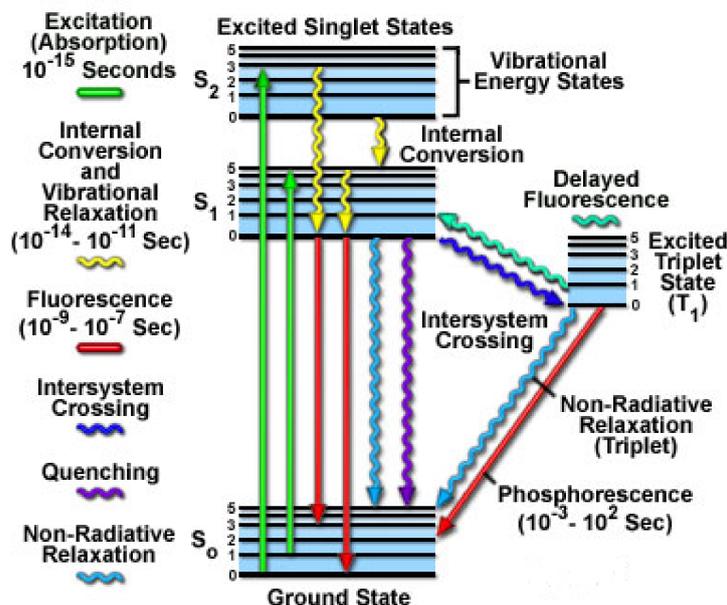
Figure 8: Jablonski Diagram of Fluorescence

Absorption of light lifts the fluorophore into an excited state (green arrows). The molecule may relax into the S1 state (yellow arrows). From the S1 state, the fluorophore can either emit a photon and return to its ground state, or first go to its triplet state T1 (also called dark state) and then to its ground state by emitting a photon.

Image adapted from [14].

ing only between S1 and the ground state. This effective reduction of emission light can result in often unwanted blinking of the fluorophores, giving the triplet state the synonym *dark state*.

There are different kinds of fluorophores; organic fluorophores, fluorescent proteins, and quantum dots, and different strategies to label the molecule of interest with them:

1. **Binding partners:** Binding partners of the proteins of interest can be fluorescently labeled. In this work, the organic fluorophore AlexaFluor^{TM}647 linked to the actin-binding protein phalloidin was used to label actin.

2. **Immunostaining:** In this case, the binding partner is an antibody or a part of an antibody (Fab fragment). The GPI-anchored membrane protein CD59 was labeled in this work with an antibody Fab fragment conjugated to the fluorophore CF^{TM}640R.

3. **Fluorescent fusion proteins:** With the help of genetic manipulation, cells can be forced to produce a fluorescent version of a protein, where the protein of interest is fused to an intrinsically fluorescent protein such as GFP. These so-called fusion proteins can either be the protein of interest or its binding partner. The latter approach was used in this work when labeling actin with the actin-binding fusion protein Utrophin-mEos3.2 or LifeAct-GFP. Fusion proteins are often used to visualize proteins within the cytoplasm or at the inner side of the plasma membrane, because there is no need to fix and permeabilize the cell membrane.

1.6 Microscopy

To image fluorescently labeled cells, the fluorophores have to be excited with a wavelength within the excitation spectrum of the fluorophores. The emitted light has then to be focused onto a camera chip to create a recordable image. There are various ways to achieve this; most of the methods, including the one used in this thesis, illuminate and image through the same objective (epifluorescence).

In epi-configuration, the excitation light excites fluorophores in the whole sample. The fluorophores near the focal plane are focused onto the camera chip, the ones farther away lead to an increase in background signal. The excitation of out-of-focus fluorophores and auto-fluorescent particles is often unwanted since it decreases the signal-to-noise ratio and increases bleaching and phototoxicity.

A variety of strategies to deal with this issue are based on reducing the illumination volume and/or imaging volume. Here, total internal reflection fluorescence (TIRF) microscopy was used for imaging. The principle of TIRF microscopy is shown in the right panel of Figure 9. The illumination light enters the objective parallelly to the optical axis, but not centrally. The distance to the center defines the angle in which the light exits the objective. If this angle is big enough, the light is totally reflected at the surface of the coverslip carrying the sample, creating an evanescent field with exponentially decreasing intensity in the sample. This allows one to only observe fluorophores within a distance of around 150 nm from the glass surface.
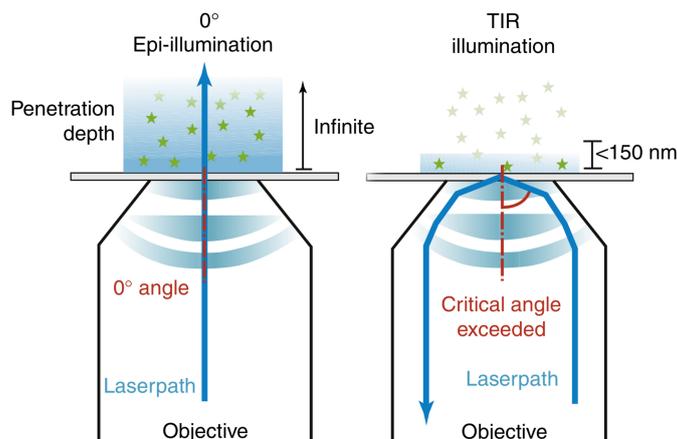
Figure 9: Illumination Strategies

In epi-illumination (0°), fluorophores throughout the sample are excited. By moving the illumination beam away from the center of the objective, the angle between the beam and the glass increases. At the critical angle, the beam gets totally reflected, creating an evanescent field with exponentially decreasing intensity in the sample. Image adapted from [8].

This distance is sufficiently large to illuminate the plasma membrane (~4 nm) at the glass surface and the associated cytoskeleton, but small enough to avoid excitation of the autofluorescent nucleus or the fluorophores located in the cytoplasm, the endoplasmatic reticulum, or the plasma membrane on the top side of the cell.

1.7   Staining Actin

Different methods were used to stain the actin skeleton. Figure 10 shows how the different molecules used bind to actin fibers.

1.7.1   Phalloidin

Phalloidin is a toxin found naturally in death cap mushrooms. It binds and stabilizes filamentous actin. A variant tagged with the organic fluorophore AlexaFluor™647 (Phalloidin-Alexa647) was used to label actin.
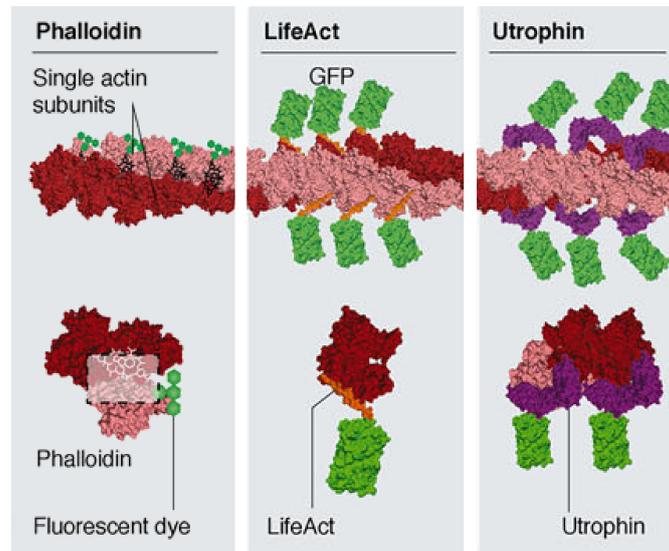
Figure 10: Different Actin Stains bound to Actin

Depicted are surface reconstructions of actin monomers (red and pink) forming an actin filament and the different actin labels with there fluorophores (green) binding to it. [15].

Phalloidin-Alexa647 cannot pass the plasma membrane, thus two different strategies were used to achieve efficient labeling: a) Phallodin-Alexa647 was introduced into cells after cell fixation and permeabilization of the plasma membrane (see Section 2.3) or b) the top plasma membrane was removed by sonication (see Section 2.5).

1.7.2   LifeAct and Utrophin

LifeAct (a peptide) and Utrophin (a protein) use actin-binding domains to bind to actin fibers and are fused to a fluorescent protein. Transient transfection was used to introduce plasmid DNA into the cells coding for LifeAct-GFP and Utrophin-mEos3.2, one day before measuring actin (see Appendix A.3). mEos3.2 is a photo-switchable fluorescent protein, which changes its absorption and emission spectrum after "switching" it irreversibly with an UV laser pulse.

1.8   Cell Lines

The cells used in this work were immortalized cell lines which are able to live and divide *in vitro* and so can be cultivated in cell culture (for protocols see Appendix A.1). Two different types of cells, HeLa and Jurkat cells, were used:

HeLa cells are named after their donor Henrietta Lacks. The cells originated from a cancerous cervical tumor and are the first cell line established from human cells. The cells are epithelial cells and so naturally tend to adhere to surfaces.

Jurkat cells originate from cancerous human T-lymphocyte cells. These cells are white blood cells and therefore non-adhesive. This means they have to be cultured in a suspension cell culture. The non-adhesive character of these cells can also lead to unwanted detaching phenomena during experiments.

Plasmids carrying the genes coding for GFP-TM-Ezrin and GFP-TM-Ezrin* were introduced into both cell types using retroviral infection to create four different cell lines (for protocol see Appendix A.2).

2   Materials and Methods

2.1   Microscope Setup

A cartoon of the microscope setup used is shown in Figure 11. During this work, different lasers were used for excitation: a 674 nm (red) diode laser (Toptica iBeam smart 200mW), a 532 nm (green), a diode-pumped solid state laser (Spectra physics Millennia 6s), a 488 nm (blue) diode laser (Toptica iBeam smart 200mW), and for fluorophore activation a near UV light 405 nm ion laser (Coherent Innova 90C). The beam profile was shaped into a Gaussian beam by spatial filtering, where the beam is focused through a pinhole, and then collimated again by a second lens. The beam diameter can be tuned by changing the lens constellation of the spatial filter. The two colored excitation beams were merged into one beam by the use of multiple dichroic mirrors. A second set of lenses was used as a telescope to focus the beam onto the back focal plane of the objective. The beam was coupled into a Zeiss microscope (Axiovert 200 inverted microscope) via two mirrors

which function as a periscope. One mirror is movable and allows for a parallel movement of the beam, which is necessary for TIRF microscopy (see Section 1.6).

Before the excitation beam enters the objective, it gets reflected by a dichroic mirror, which is designed in such way that it reflects the wavelength of the excitation beam but lets the Stokes-shifted emitted light pass through, allowing one to separate the emitted light. After passing the dichroic mirror, the emitted light is filtered to reduce stray light from the excitation beams, and split into multiple color channels (Cairn Research Optosplit), which are projected onto non-overlapping parts of the camera chip, allowing for multi-color imaging.

Although TIRF illumination was used for all measurements, epi-illumination was used for imaging preparation and whole-cell observation.
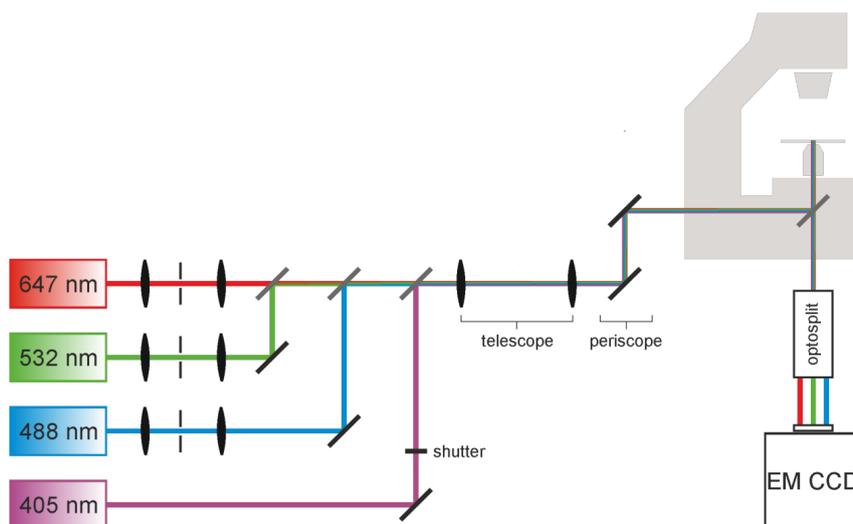

Figure 11: Cartoon of the Used Microscope Setup
The lasers are overlaid and coupled into the microscope to excite the specimen. The fluorescence light is filtered, split into different color channels and focused onto the camera. Both excitation and emission beams pass through the same objective and are separated by a dichroic mirror. Figure adapted from [16].

2.2   Protocols for Micropatterning

2.2.1   Micropatterning Protocol Developed in Our Laboratory
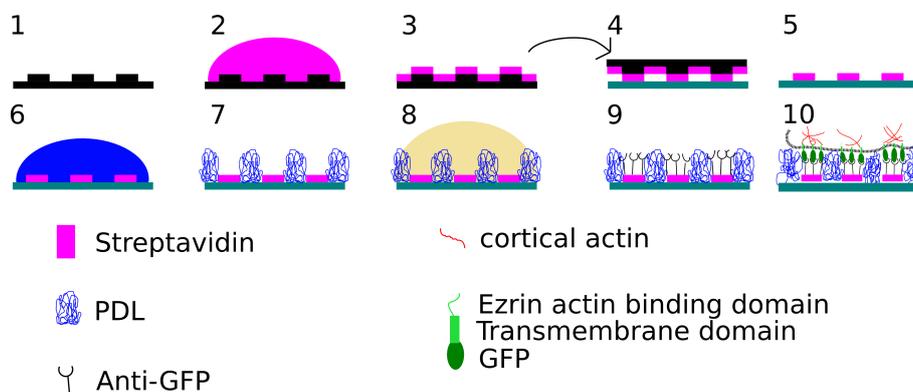

Figure 12: Stamping Procedure

The figure displays the steps to prepare the coating of the glass slides used to pattern the actin inside the cells. 1: cleaned and dried stamp, 2: incubating with streptavidin, 3: removing excess streptavidin and drying with N$_2$, 4: stamping of streptavidin onto epoxy-coated glass slide, 5: removal of stamp, 6: incubation with FN, BSA or PDL, 7: rinsing of the glass surface with 1x phosphate-buffered saline (1×PBS), 8: incubation with GFP antibodies, 9: rinsing with 1×PBS, 10: incubation with cells in appropriate cell media.

In this thesis, polymer stamps were used to create a protein pattern on a coverslip glass surface. Depending on the pattern size, two different materials were used. The stamps with the bigger structures ($\geq$ 1 µm) were made of polydimethylsiloxane (PDMS), the stamps with finer structures were made of a proprietary polymer material ("material 1") provided by our industrial partner EV-Group. The protocol differs slightly for the two materials. An overview of the procedure can be seen in Figure 12.

1. **Cleaning the stamps:** Rinsing the stamps, first with ethanol and then with ultra-pure water. Drying the stamp under a stream of N$_2$.

2. **Incubation of stamps with streptavidin:** Diluting streptavidin with ultra-pure 1×PBS to 50 $\frac{\mu g}{ml}$. Covering the patterned region of the stamp with a drop of the solution and incubating for 10 minutes.

3. **Removing excess streptavidin:** PDMS stamps: rinsing the stamps with ultra-pure water and drying with an N_2 stream.
   Material 1 stamps: the rinsing step was omitted.

4. **Stamping of pattern onto glass slide:** Placing the patterned side of the dried stamp onto the epoxy-coated glass slides (Schott). Leaving the stamps on the glass slides for five minutes.

5. **Removing the stamps:** Marking the patterned area on the back of the glass slide with a waterproof pen and carefully removing the stamp. Placing a chamber (Secure Seal hybridization chambers) over the patterned region. Line stamps: placing chamber to align chamber openings with the pattern.

6. **Filling with the background coating:** Filling the chamber with the background coating material, incubating for 30 minutes. (1% BSA or 50 $\frac{\mu g}{ml}$ fibronectin or 50 $\frac{\mu g}{ml}$ PDL)

7. **Removing excess background coating:** Rinsing the chamber with 1×PBS.

8. **Incubating with antibodies:** Incubating with biotinylated GFP-antibodies dissolved in 1×PBS with 1% BSA (to avoid unspecific binding) for 15 minutes.

9. **Removing excess antibodies:** Carefully rinsing the chamber with 1×PBS.

10. **a) To image cells:** Filling the chamber with cells suspended in culture medium and incubating at 37 °C and 5% CO_2) until cells adhered to the surface (approx. 15 minutes on FN and 45 minutes on PDL). Cells were measured in their medium.

    b) To image pattern: Incubating cells at 37 °C in HT-GFP (0.1 μM in 1×PBS) for 2 minutes. Removing excess HT-GFP by rinsing the chambers with 1×PBS.

2.2.2   Micropatterning Protocol Developed in Jacob Piehler's Group

The patterning strategy used by Jacob Piehler [6] was replicated. Figure 13 shows the assembled pattern. PLL-PEG-HTL, PLL-PRG-HTL, PLL-PEG-RGD and HT-GFP were a gift from J. Piehler, U. Osnabrück, which we gratefully acknowledge.
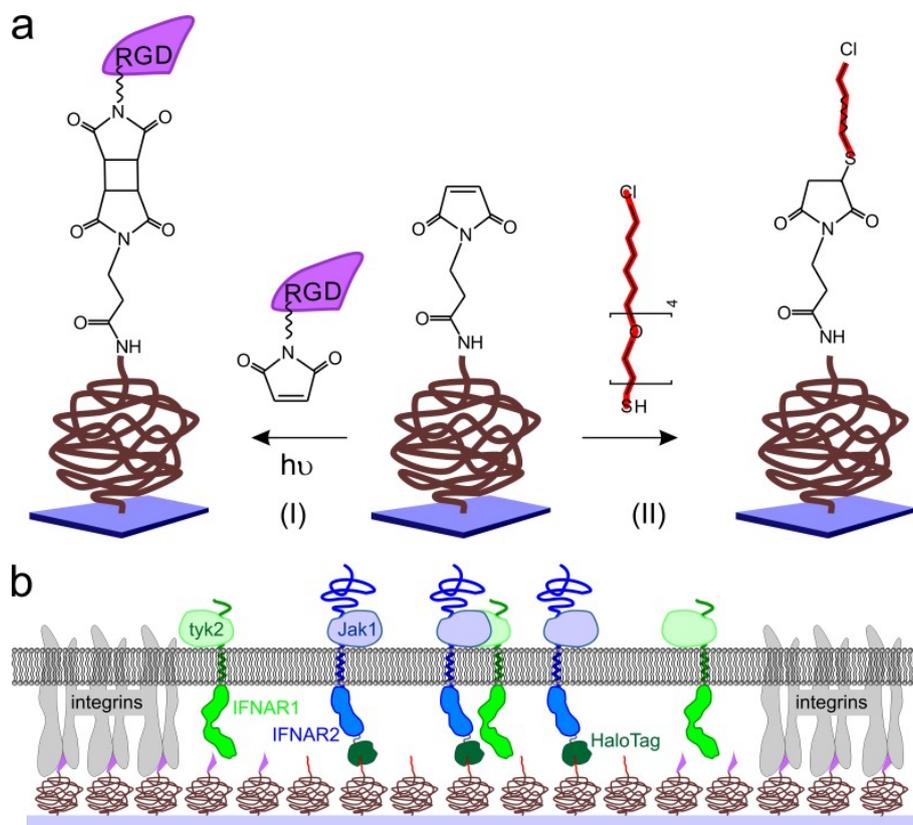
Figure 13: Micropatterning Protocol Developed in Jacob Piehler's Laboratory

a: *PLL-PEG fused to an RGD protein (left) and an HTL (right)*

b: *Cartoon of the assembled pattern; RGD bound to the integrins of the cell (on the sides) and HTL bound to the HT of the constructed transmembrane protein. Figure taken from [6].*

1. **Plasma cleaning of coverslips:** Treating glass coverslips with air plasma for 10 minutes.

2. **Incubating stamps with PLL-PEG-HTL:** Wetting the stamps with PLL-PEG-HTL (0.5 mg/ml in 1×PBS) and incubating for 15 minutes.

3. **Removing of excess PLL-PRG-HTL:** Rinsing the stamps with 1×PBS and ultra-pure water, drying with N_2 air blower.

4. **Stamping of pattern onto glass slide:** Gently pressing the patterned side of the dried stamp onto the coverslip using the thumb. Leaving the stamps on the glass slides for 30 minutes to incubate.

5. **Removing the stamp:** Removing the stamp carefully using tweezers.

6. **Backfilling with PLL-PEG-RGD:** Wetting the patterned glass slide with PLL-PEG-RGD (2% PLL-PEG-RGD (0.002 mg/ml) and 98% PLL-PEG (0.1 mg/ml) dissolved in 1×PBS) for 10 minutes to backfill the patterned structure.

7. **Removing of excess PLL-PEG-RGD:** Rinsing with 1×PBS and drying with a stream of N_2.

8. **a) To image pattern:** incubating with HT-GFP (0.1 μM in 1×PBS) for two minutes at 37 °C, rinsed with 1×PBS.

   b) To image cells: incubating with HT-antiGFP (30 nM in 1×PBS) for two minutes at 37 °C, rinsing with 1×PBS, seeding the GFP-TM-Ezrin-expressing cells on the pattern and incubating at 37 °C and 5% CO_2 until they adhere (~30 minutes). Cells were measured in their medium.

2.3   Fixing and Permeabilizing Cells

2.3.1   Fixing Cells

Para-formaldehyde (PFA) was used to fix the cells. Since PFA fumes are toxic, it has to be handled under a chemical hood.

1. incubating cells in chambers on cover slip in their respective medium in the incubator at 37 °C, 5% CO_2, and high humidity until they adhere

2. washing cells gently with 1×PBS

3. removing 1×PBS from chamber and filling it with 4% PFA in Hank's Balanced Salt Solution (HBSS)

4. incubation at room temperature for exactly 10 minutes

5. discarding PFA in designated trash

6. washing with 1×PBS (also discarded along with PFA since there are still residuals)

7. incubating with BSA for 30 minutes

2.3.2   Permeabilizing the Plasma Membrane

The plasma membrane of already-fixed cells can be permeabilized, allowing substances to enter the cell which can not pass through intact plasma membranes. This was achieved by incubating fixed cells with 0.1% Triton X-100 for 10 minutes and then with 10% BSA for 30 minutes.

2.4   Staining Actin with Phalloidin

Cells with ripped or permeabilized cell membrane were incubated with phalloidin-Alexa647 dissolved in BSA (200 U phalloidin-Alexa647 in 400 µl BSA) for 5 minutes. Excess phalloidin-Alexa647 was removed by rinsing with 1×PBS.

2.5   Removal of Cell Body by Sonication

The cells were incubated on patterned coverslips in chambers made from cut Eppendorf tubes or alternatively in secure seal chambers without altering the outcome significantly. The adherence of the cells was checked by observing them under the TIRF microscope.

Sonication was then used to remove the top membrane, cell body and stress fibers. A Branson Digital Sonifier Model 450 (Branson, Connecticut, USA) with a maximum power of 400 W was used as a sonicator. An isotonic solution with 70 mM KCl, 30 mM HEPES, 5 mM MgCl2, 3 mM EGTA, pH 7.5 was used as soni-buffer (all added chemicals were purchased from Sigma-Aldrich, Missouri, USA))

1. cooling 100 ml 1×PBS to 0 °C

2. preparing "hypo-buffer" by mixing $\frac{2}{3}$ H$_2$O with $\frac{1}{3}$ soni-buffer

3. exchanging the liquid twice with ice-cold 1×PBS

4. exchanging the liquid three times with hypo-buffer

5. exchanging the liquid with soni-buffer

6. filling a beaker with soni-buffer, and placing a chamber inside

7. adjusting the sonicator tip to be 1-2 mm under the buffer surface

8. applying two 0.2-second-long pulses with 0.2-0.5 second breaks in between at 15% of the maximum intensity

2.5.1   Staining the Plasma Membrane

To control for an intact plasma membrane, the remaining plasma membrane was stained by immunostaining CD59, a GPI-anchored protein, with an antibody Fab fragment conjugated to the fluorophore CF^{TM}640R (10 $\frac{\mu g}{ml}$, 10 minutes in medium).

3   Results

The goal of this work was to create a well-defined pattern of the cortical actin in live cells. To achieve this goal, we first optimized the separation of active and background coating ("A" and "B" in Figure 5) to improve the contrast between "on-pattern" and "off-pattern" areas.

Then, the quality of patterns formed by the GFP-TM-Ezrin protein and the GFP-TM-Ezrin* protein in the plasma membrane was evaluated on different surfaces. Finally, different methods to image the cortical actin patterns were tested and optimized.

3.1   Optimization of Micropatterning Protocols

Three different approaches were used in this work to create micropatterned glass surfaces:

1. printing of streptavidin and backfilling with FN

2. printing of streptavidin and backfilling with PDL

3. printing of PLL-PEG-RGD and backfilling with PLL-PEG-HTL following a protocol developed by Jacob Piehler's group [6]

The brightness of the GFP signal in "on-pattern" areas (I_{on}) and "off-pattern" areas (I_{off}) was used to calculate the contrast $C = \frac{I_{\text{on}} - I_{\text{off}}}{I_{\text{on}}}$ of stained patterns, as well as patterns imaged in cells.

3.1.1 Optimization of Pattern Quality

Calculating the contrast of the patterns created using the different patterning protocols showed no clear difference between them. The results are summarized in the central column of Table 1.

The rinsing steps in the protocol were optimized for stamps featuring lined structures by rinsing parallel to them and some rinsing steps were omitted for all stamps in order to reduce patterning artifacts like the "ear-like" artifact (Figure 14). These optimizations are included in the protocols which can be found in Section 2.2.

Protocol:	only pattern	HeLa cells
Piehler	0.75	0.8[*]
ours with PDL	0.8	0.7[**]
ours with FN	0.7	0.6[*]

*Table 1: **Comparison of Contrast Using Different Patterning Protocols***
The indicated contrast values were calculated each from 3 different cells on different slides, and the values for "only pattern" from 2-4 different slides. 3 μm-sized circular pattern were used unless indicated otherwise. [*]These measurements were done on the same day with cells of the same passage number. [**]1 μm-sized circular patterns and sorted cells from a higher passage number were used.

3.1.2 Adherence of Cells to Patterned Surfaces

HeLa cells tended to adhere more slowly to PDL-backfilled glass slides than to FN, but by incubating for half an hour longer (45 minuted total), cells spread to cover nearly the same surface area as on FN. On both background coatings, media exchange was possible without detaching the cells.
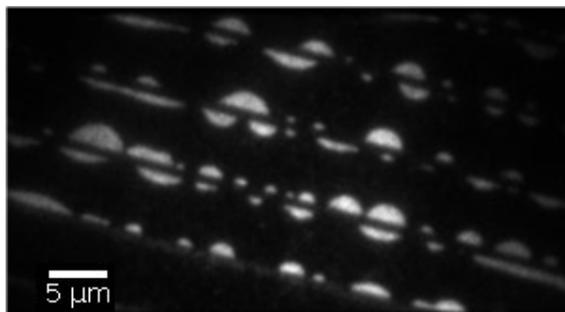
Figure 14: Ear-like Artifact in Line Patterns

Stamps featuring line patterns (1 μm wide, 5 μm distance) sometimes formed these ear-like artifacts. Their occurrence could be reduced by always rinsing the stamp parallelly to the line structure of the stamp. The pattern was created using our protocol and PDL as background filling. The pattern was stained using HT-GFP (green channel).

With BSA, on the other hand, cells were detaching even if the liquid was exchanged very slowly and gently. Therefore, we stopped using it as background coating.

3.1.3   Effect of Different Patterning Methods on Pattern Quality in Hela Cells

After the quality of the patterns produced became quite consistent, we started seeding HeLa cells expressing GFP-TM-Ezrin on patterned surfaces.
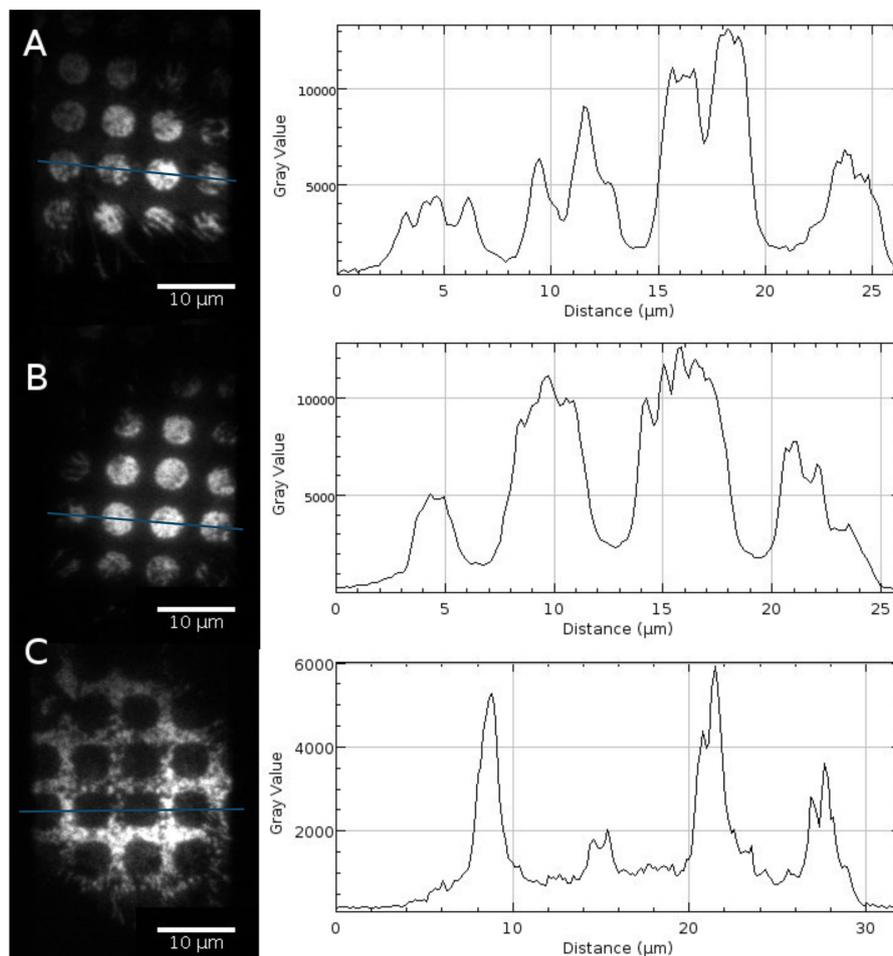
Figure 15: Representative Images of HeLa cells expressing GFP-TM-Ezrin on Patterns Made According to Jacob Piehler's Protocol

HeLa cells expressing GFP-TM-Ezrin were seeded onto a surface patterned following the protocol established in the laboratory of Jacob Piehler. GFP was imaged using TIRF microscopy. A, B and C show cells on different slides; in C, a differently designed stamp was used. On the right, brightness profile along the blue line of the corresponding cell is displayed. The lines are chosen such that they are close to the center of illumination and pass through the center of the active coating.

Figure 16: Representative Images of HeLa Cells Expressing GFP-TM-Ezrin on FN Patterns
This figure is similar to Figure 15, except that the cells were seeded onto a pattern created following the protocol developed in our laboratory using FN as background coating. Note the lower contrast compared to Figure 15.

A measurement series of HeLa cells expressing GFP-TM-Ezrin on patterns, produced by following Jacob Piehler's protocol (see Figure 15) and following our protocol using FN as background coating (see Figure 16), was performed. These series were produced on the same day with cells from the same passage and the same microscopy settings, and by using stamps having similar layouts, making a direct comparison of the two possible. The calculated contrast was higher using Jacob Piehler's protocols (contrast ~0.8) than when using our protocols and FN (contrast ~0.6).
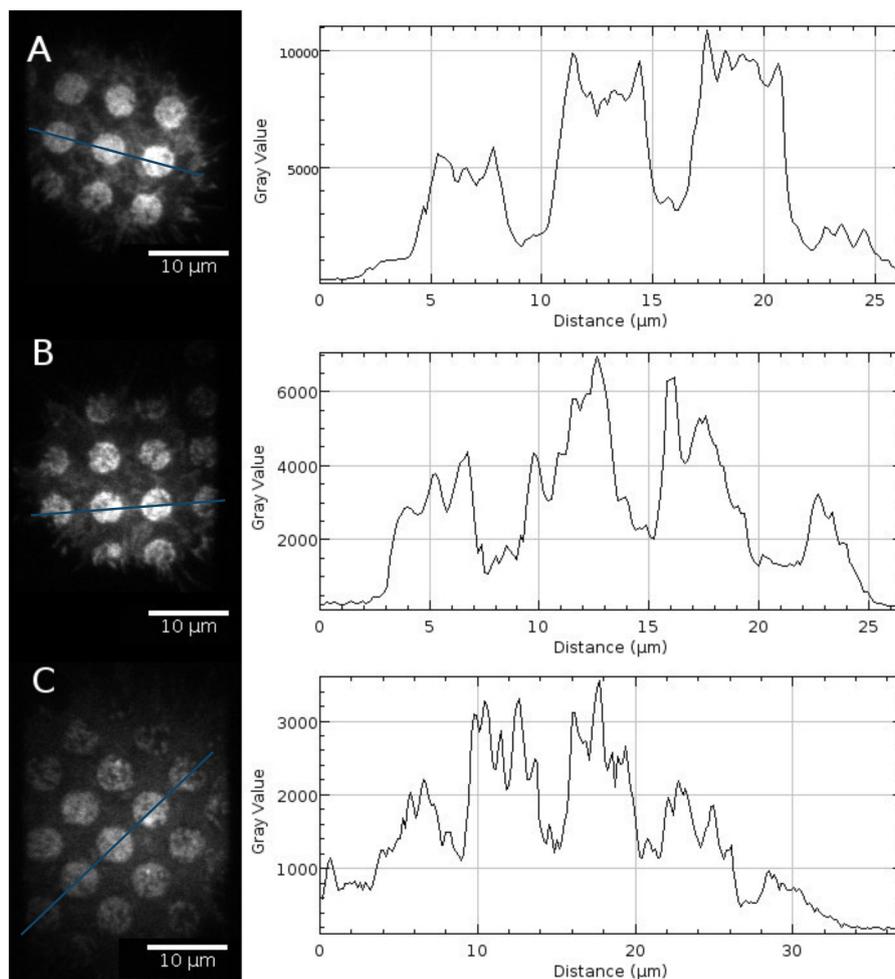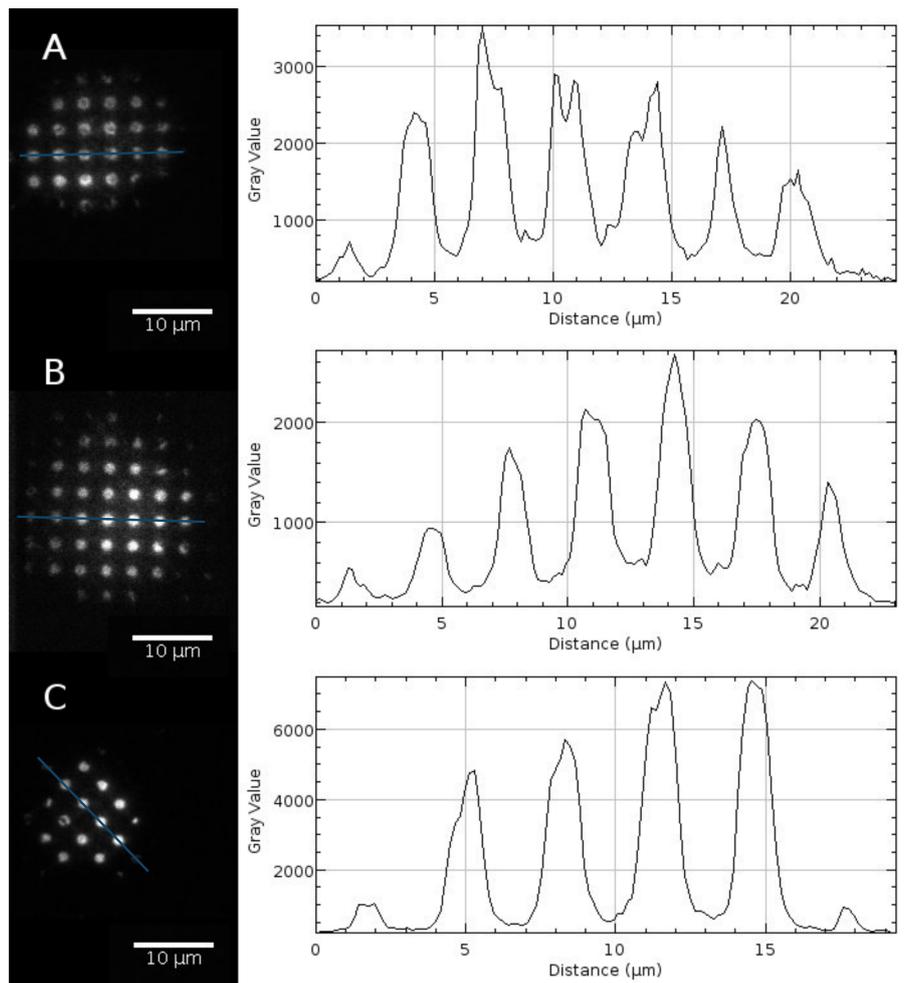
Figure 17: Representative Images of HeLa Cells Expressing GFP-TM-Ezrin on PDL Patterns
This figure is similar to Figure 16, except PDL was used as background coating, and that stamps had a smaller pattern size. These measurements were done multiple cell passages and after sorting the cells for high expression levels of GFP-TM-Ezrin. As such, this result is not directly comparable to the others.

Due to this result, and to avoid promotion of actin polymerization "off-pattern" due to integrin binding, we changed our protocol to use PDL as background coating. Examples of HeLa cells expressing GFP-TM-Ezrin can be seen in Figure 17. In these experiments, stamps with smaller pattern size were used (contrast ~0.7).

3.1.4   Effect of Stamp Layouts on Pattern Quality in Hela Cells

While producing homogeneous patterns with high contrast in the preliminary experiments, where patterns were stained with HT-GFP, the stamps featuring larger patterns (diameter of 3 μm, 35% of surface area is "on-pattern") tended to produce pronounced intensity inhomogeneities within the circular GFP-TM-Ezrin patterns in HeLa cells. The most likely explanation for this was insufficient GFP-TM-Ezrin expression for the amount of antibody that was available for GFP binding.

Therefore, stamps with a smaller pattern size (diameter of 1 μm, 17% of surface area is "on-pattern") were tested, where the decreased "on-pattern" area should compensate for the low GFP-TM-Ezrin expression levels (summarized in Table 2). The GFP-TM-Ezrin expression was also increased by sorting the cells for high expression levels using fluorescence assisted cell sorting (FACS).

1 μm stamps usually yielded a better pattern quality than 3 μm stamps and line patterns. Thus, the following experiments were mainly conducted using 1 μm stamps, although in cases of low contrast, or structured background signal, line patterns can have the advantage of being more easily recognized than circular ones.

Stamp used:	
lines	17% active coating; easier to observe in cells; more prone to artifacts
1 μm circle	17% active coating; high density
3 μm circle	35% active coating; density inhomogeneities

*Table 2: **Remarks on Stamp Types***

3.2   Patterned Actin in HeLa Cells

The next step was to check whether patterning of GFP-TM-Ezrin in fact led to a reorganization of cortical actin to patterned regions. To get direct information about the local actin density, actin was labeled using different strategies.

3.2.1   Comparison of Different Methods to Label Actin

Phalloidin is considered the gold standard for visualizing actin in cells. HeLa cells expressing GFP-TM-Ezrin and GFP-TM-Ezrin* were seeded onto patterned glass surfaces. The cells were fixed and their membranes permeabilized following the protocol in Section 2.3. Phalloidin-Alexa647 was used to label the actin skeleton.

Unfortunately, actin patterns that were clearly following the micropatterned GFP-TM-Ezrin template could only be observed in two of the dozens of cells imaged. In all other cells, actin stress fibers dominated the images. Due to the thickness of stress fibers, it is likely that the majority of phalloidin-Alexa647 is bound to the fibers rather than to patterned cortical actin. One of the two cells where a pattern was visible is shown in Figure 18.

Figure 18: GFP-TM-Ezrin-Expressing HeLa Cells with Phalloidin-Alexa647 Actin Stain
HeLa cells expressing the GFP-TM-Ezrin protein were seeded onto a surface patterned following the patterning protocol established in our laboratory using PDL as background coating. The GFP pattern (green channel on the right) and the phalloidin-Alexa647-stained cortical actin (red channel on the left) were imaged simultaneously using TIRF microscopy. The figure shows one of two cells in which an actin pattern was visible. In most other cells observed, the stress fibers dominated the image to an extent that made it impossible to judge whether the actin in the cell was patterned at all.

Utrophin has a different underlying mechanism of binding to actin. Differences in labeling intensity, compared to phalloidin, were reported for parts of the actin skeleton [17]. That is why HeLa cells expressing GFP-TM-Ezrin and GFP-TM-Ezrin* were transiently transfected to also express Utrophin-mEos3.2 (see Figure 19). However, Utrophin-mEos3.2 also stained the stress fibers of HeLa cells and hence made an observation of the patterned cortical actin impossible.
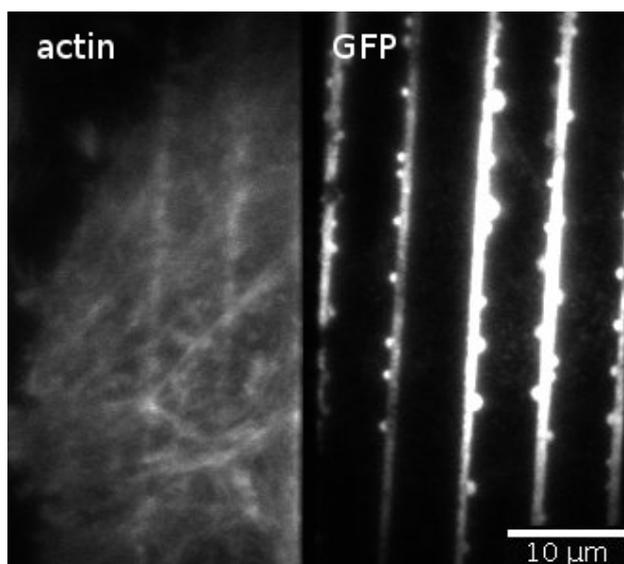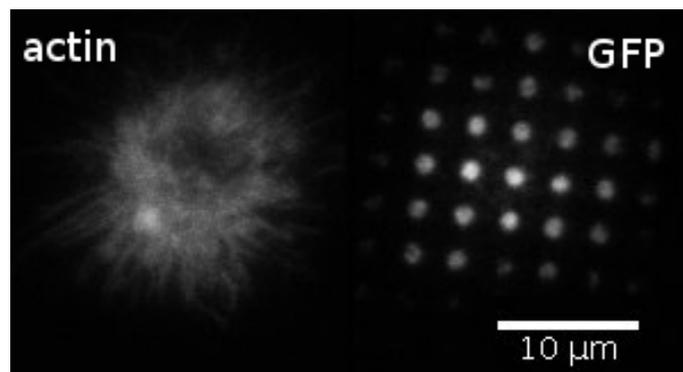

Figure 19: GFP-TM-Ezrin-Expressing HeLa Cells with Utrophin-mEos3.2 Actin Stain
HeLa cells expressing the GFP-TM-Ezrin protein were seeded onto a surface patterned following the patterning protocol established in our laboratory using PDL as background coating. The fluorescent protein mEos3.2 was switched with an intense UV (405 nm) laser pulse to be excitable with the green laser. The GFP pattern (on the right) and the Utrophin-mEos3.2-stained cortical actin (on the left) were imaged simultaneously using TIRF microscopy. The stress fibers produced by the HeLa cells made the pattern of actin nearly invisible.

LifeAct, an actin-binding peptide, has been reported to have imperfections regarding its ability to stain some types of stress fibers [18]. LifeAct-GFP was transiently expressed in HeLa and CHO cells to test for its staining of stress fibers in these cell lines. In both cases, a high amount of stress fibers was observed in the cells. Therefore, also this staining technique was found to be unsuitable to visualize the patterned actin.

3.2.2   Sonication of HeLa Cells to Remove Stress Fibers

As a next step, it was important to test whether actin-patterning via GFP-TM-Ezrin worked in cells where only stress fibers were visible when using the staining techniques men-
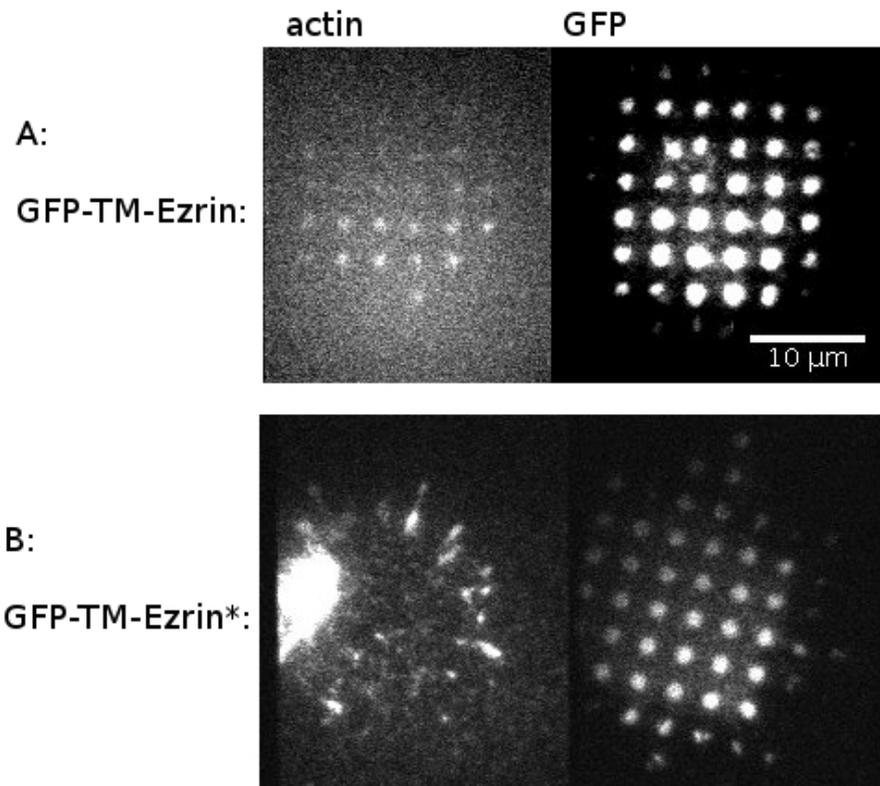
Figure 20: GFP-TM-Ezrin- and GFP-TM-Ezrin*-Expressing HeLa Cells after Sonication
HeLa cells expressing GFP-TM-Ezrin (A) and GFP-TM-Ezrin* (B) were seeded onto a surface patterned following the protocol established in our laboratory using PDL as background coating. The already-adhered cells were sonicated and the actin skeleton stained with phalloidin-Alexa647 (red channel on the left). The GFP pattern was also imaged (green channel on the right). While a phalloidin-Alexa647 actin pattern could be observed in the GFP-TM-Ezrin-expressing cells, only filopodia actin was detected in the GFP-TM-Ezrin*-expressing cells.

tioned above. Experiments in the lab indicated that sonication with a tip sonicator could be a suitable method to remove stress fibers in HeLa cells.

HeLa cells expressing GFP-TM-Ezrin and GFP-TM-Ezrin* were seeded onto patterned surfaces. This protocol was used with and without secure seal chambers with no significant difference in the result. After the cells adhered well to the surface, an isotonic buffer was used to inflate them, and sonication pulses were used to rip the cell membrane off. The protocol was optimized to set the amplitude and duration of the pulses to a minimum to keep the bottom cell membrane intact, but high enough so that the majority of

the cells on the glass slide lost their upper cell body (a detailed protocol can be found in Section 2.5).

Staining the actin with phalloidin-Alexa647 showed that sonication had yielded the desired result of removing the actin stress fibers while allowing observation of the actin pattern templated by GFP-TM-Ezrin. One of the observed HeLa GFP-TM-Ezrin cells is shown in Figure 20 A. The exact same procedure was repeated with the cells expressing the mutated protein GFP-TM-Ezrin*, which should not bind to actin. Indeed, after sonication the cells had nearly no actin left on the surface, and any actin remaining was filopodia actin and not located in the patterned areas, as can be seen in Figure 20 B.
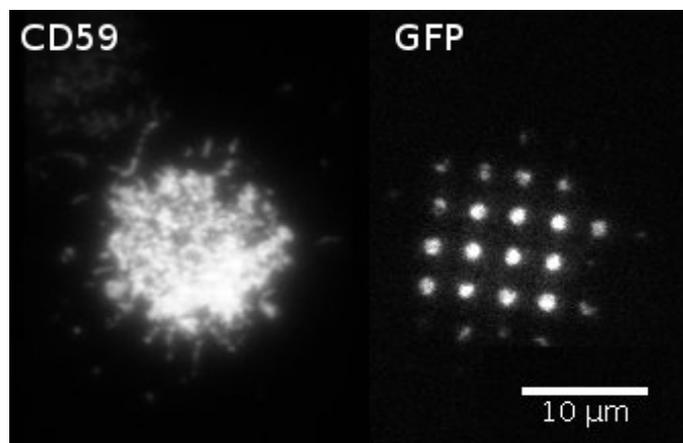
Figure 21: Stained Membrane of GFP-TM-Ezrin-Expressing HeLa Cells after Sonication
HeLa cells expressing GFP-TM-Ezrin were seeded onto a surface patterned by following the protocol established in our laboratory using PDL as background coating. The already-adhered cells were sonicated and the residual plasma membrane stained with a fluorescnetly labeled Fab fragment against CD59 (red channel on the left). The majority of the plasma membrane is still intact after sonication. The GFP pattern is shown on the right (green channel).

To check for the possibility that the observed actin patterns were an artifact due to partial detachment of the plasma membrane, the plasma membrane was stained using an anti-CD59 Fab fragment labeled with CF^{TM}640R to label CD59, a GPI-anchored protein, which should show a random distribution in the plasma membrane. We found that the majority of the bottom plasma membrane was still intact after sonication; a representative image is shown in Figure 21.

These experiments ascertained that the actin pattern in HeLa cells were actually a consequence of the patterning of GFP-TM-Ezrin and, thus, that the enrichment and reorganization of cortical actin had been successful. Further, we could prove that the observed pattern was not an artifact due to partial detachment of the plasma membrane. The actin pattern found after sonication was weak, maybe because part of the patterned actin was removed during sonication too, making a quantitative analysis of the pattern unfeasible.

3.3 Patterned Actin in Jurkat Cells

Our aim was to establish a system which enables one to relate the diffusion behavior of proteins and lipids in live cells to the local actin concentration. This was found to be infeasible in HeLa cells, since the staining of stress fibers made it impossible to determine the local actin concentration in living cells. We therefore decided to switch to Jurkat cells, a cell line reported to lack stress fibers [19].

Two stable cell lines were created by transfecting Jurkat cells to express the same GFP-TM-Ezrin and GFP-TM-Ezrin* proteins as in HeLa cells. To observe the actin skeleton, the cells were fixed, permeabilized, and stained with phalloidin-Alexa647. No stress fibers were visible and the patterns could be observed. Unfortunately, the results obtained with GFP-TM-Ezrin and GFP-TM-Ezrin* were inconsistent:

Multiple GFP-TM-Ezrin*-expressing cells showed an actin pattern (see Figure 22). This could also result from partially detached cells, giving the impression of an actin pattern when using TIRF microscopy for imaging, but the patterns were also clearly visible using epi-illumination and the homogeneous background of freely diffusing GFP-TM-Ezrin* indicated well-attached cells. Furthermore, not all cells expressing GFP-TM-Ezrin showed an actin pattern; this could result from low GFP-TM-Ezrin expression levels or bad pattern quality, but no consistent trend could be observed in this respect either. A possible explanation for the observed phenomena was that GFP-TM-Ezrin-expressing cells cross-contaminated the mutant cell line, so the process of transfection was repeated, but also in some of the newly transfected cells expressing GFP-TM-Ezrin*, an actin pattern could be observed. Also, sequencing of the plasmids did not show any cross-contamination of the plasmids themselves.
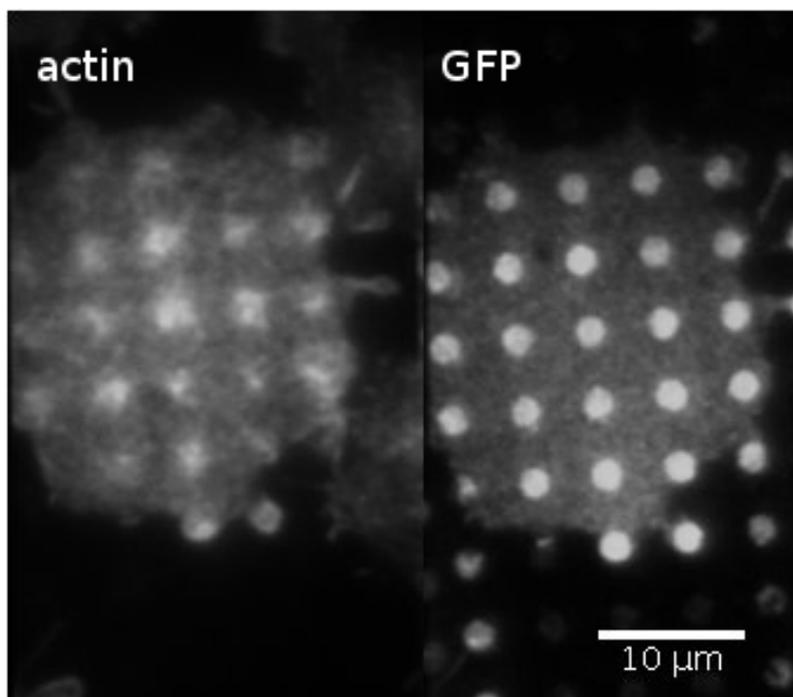
Figure 22: GFP-TM-Ezrin*-expressing Jurkat Cells with Phalloidin-Alexa647 Actin Stain
Jurkat cells Expressing GFP-TM-Ezrin* were seeded onto a surface patterned following our
protocol and PDL as background coating. They were fixed, permeabilized and stained with
phalloidin-Alexa647 (red channel on the left). The actin skeleton of the cells showed a pattern
even though Ezrin* should not be able to bind to actin. The right image shows GFP (green chan-
nel).

3.4 Transmission Electron Microscopy

In addition to fluorescence microscopy, we planned to also image the patterned actin skeleton via transmission electron microscopy (TEM) to learn about its sub-micron structure. Although this was never realized due to the above-mentioned problems with stress fibers in HeLa and possible cross-contamination in Jurkat cells, the protocol for the preparation of electron microscopy samples was developed and optimized:

The measurements were planned as collaboration with the electron microscopy facility of the Vienna Biocenter Core Facilities. To be able to image the patterned cells in TEM, it was necessary to seed them onto a a thin carbon foil supported by a metallic grid. This foil tended to rip or peel off the grid during the patterning process. This was avoided

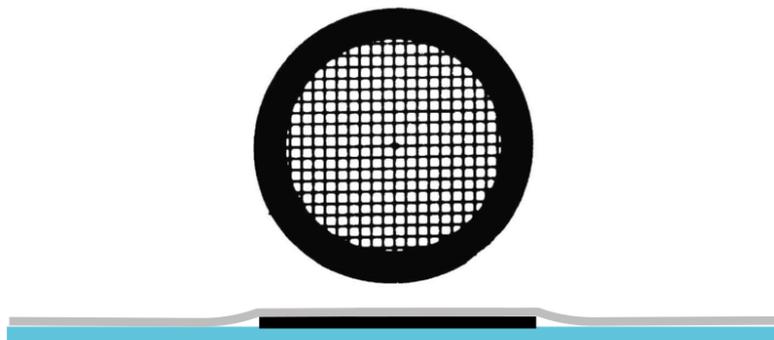***Figure 23: Assembly of Foil and Grid for Patterning***

The cartoon shows how the glass (blue) supports the carbon foil (gray) on the metal grid (black). Since the foil also covers the glass, ripping of the foil during the patterning process is less likely. Figure adapted from [20].

by not only covering the grid but also a supportive glass slide with the foil, as can be seen in Figure 23.

4   Conclusion

The aim of this work was to provide a tool to study the influence of cortical actin on the organization and dynamics of lipids and proteins in the plasma membrane. By micropatterning the cortical actin into regions of high and low actin density, it becomes possible to gain quantitative information about diffusion characteristics relative to the cortical actin density.

During this work, a protocol was established and optimized to consistently pattern GFP-TM-Ezrin and GFP-TM-Ezrin* proteins in the cell membrane. Although the stress fibers of HeLa cells prevented a direct observation of the actin pattern in intact cells, effective actin patterning via GFP-TM-Ezrin could be shown by removing the upper cell body and stress fibers using sonication. Also, no reorganization of actin was observed when the actin-binding deficient mutant was patterned. While these results proved that patterning of cortical actin, in principle, was possible via the developed approach, the HeLa cell system could not be used for the planned diffusion experiments in living cells. For Jurkat cells, where stress fibers did not obscure the produced actin patterns, results were inconsistent, as both in GFP-TM-Ezrin- and GFP-TM-Ezrin*-expressing Jurkat cells, actin patterns were present in some cells and not in others.

A likely explanation for these observations was cross-contamination of GFP-TM-Ezrin- and GFP-TM-Ezrin*-expressing cells, but thawing older passage numbers and establishing new lines by repeating the transfection did not solve this issue. Since these were very time-consuming procedures, it was not possible to measure any diffusion behavior within the time frame of this work.

The next step in this project would involve re-transfection of Jurkat cells, as well as other cell lines which do not exhibit stress fibers, with GFP-TM-Ezrin and GFP-TM-Ezrin* plasmids. For cells with low GFP-TM-Ezrin(*) expression, 1 μm circular patterns would be beneficial due to their lower "on-pattern" surface coverage. For cells with a high and structured actin background, line patterns could be of advantage since those can be identified more easily. PDL proved to be the background coating of choice, since cells adhered well to it and it did not interfere with cortical actin. Actin should be labeled using methods which do not require fixation and permeablization of cells, to allow for

observation of diffusion and actin simultaneously. Preferably, the fluorophore would be photostable and bright enough to allow for actin density measurements via single molecule brightness analysis. SiR-actin would be a possible candidate, since it is membrane-permeable, bright and photostable [15]. Replacing the GFP in GFP-TM-Ezrin(*) with a non-fluorescent domain capable of selective binding (e.g. HT) would allow using green fluorophores for other purposes such as labeling actin or proteins and lipids, making the experiment design more versatile.

A Appendices

A.1 Cell Culture

A.1.1 HeLa Cells

Two stable lines of HeLa cells, one expressing GFP-TM-Ezrin, and another expressing GFP-TM-Ezrin*, serving as a control, were used.

HeLa cells were cultured in tissue culture flasks (75 cm^2) using DMEM supplemented with 10% fetal calf serum, 2mM L-Glutamine and 1000 U/ml of penicillin/streptomycin (full suppl.). The cells were split at a 1:10 ratio every 3-4 days the following way:

1. heating all required liquids in a water bath to 37 °C (PBS, accutase and DMEM)

2. removing old medium

3. washing cells gently with 1×PBS; careful aspiration of 1×PBS

4. detaching the cells by incubating in 2 ml accutase until detached (~ 5 minutes)

5. addition of 5 ml medium (DMEM, full suppl.)

6. transferring the cell suspension into a 15 ml falcon tube

7. spinning cells down at 400×g for 3 minutes

8. removing liquid and re-suspending the cell cluster in 1 ml medium (DMEM, full suppl.)

9. seeding 100 µl of the cell suspension into the cell culture flaks with 10 ml fresh medium (DMEM, full suppl.)

10. storing the cells until their next use in an incubator at 37 °C, 5% CO_2 and high humidity

A.1.2   Jurkat Cells

Similarly to the HeLa cells, two stable lines of Jurkat cells, one expressing GFP-TM-Ezrin and another GFP-TM-Ezrin*, serving as a control, were used.

Jurkat cells are suspension cells and were cultured in culture flasks using RPMI 1640 medium supplemented with 10% fetal calf serum, 2mM L-Glutamine and 1000 U/ml of penicillin/streptomycin (full suppl.). Every 3-4 days, half of the cell suspension was removed with a pipette and discarded. The same amount of fresh medium (RPMI, full suppl.) heated to 37 °C was added to the flask. The cells were incubated in flasks in upright position in an incubator at 37 °C, 5% CO_2, and high humidity.

Every second week, the medium was completely changed. This was done by spinning the cells down (400×g for 3 minutes), aspirating the old medium, resuspending the cells in fresh medium and transferring half of the cells to a new flask with fresh RPMI medium.

A.2   Viral Transfection of Jurkat Cells

To create a stable cell line of Jurkat cells expressing GFP-TM-Ezrin or GFP-TM-Ezrin*, first, Φnix cells were transfected with a plasmid containing the respective gene, flanked by viral sequences and plasmids encoding for viral helper proteins. The transfected Φnix cells produced a virus, containing the plasmid coding for the GFP-TM-Ezrin or GFP-TM-Ezrin* protein, which was used to infect the Jurkat cells.

1. **Detachment of Φnix cells:** Using 70% confluent Φnix cells in T75 flasks.

    (a) removing old medium

    (b) washing cells gently with 1×PBS; carefully aspirating 1×PBS

    (c) detaching the cells by incubating in 2 ml accutase until detached ($\sim$ 5 minutes)

    (d) addition of 5 ml medium (DMEM, full suppl.)

    (e) transferring the cell suspension into a 15 ml falcon tube

    (f) spinning cells down at 400×g, 3 minutes

    (g) removing liquid and re-suspending in 1 ml medium (DMEM, full suppl.)

2. **Seeding Φnix cells:** Using three 10 mm tissue culture Petri dishes coated for tissue culture for each transfection:

    (a) filling 10 ml medium (DMEM, full suppl.) in each Petri dish

    (b) seeding cells into the Pertri dish, with density to reach 70% confluency after incubating overnight at 37 °C, 5% CO_2 and high humidity

3. **Transfection of Φnix cells:** preparation of the DNA transfection reagent complex:

    (a) pipetting 66 μl Fugene centrally into an Eppendorf tube with 1 ml opti-MEM, vortexing immediately and letting solution sit for 5 minutes

    (b) adding a mixture of 17 μg of the plasmid of interest, 12 μg pgag-pol and 4 μg pMD2.G to the solution and vortexing immediately

    (c) incubating the solution for 15 minutes at room temperature

    (d) adding the solution to the cells by carefully dripping the solution onto them

    (e) incubating at 37 °C, 5% CO_2 and high humidity

    (f) changing the medium (DMEM, full suppl.) after 5 hours and continuing incubation for two days

4. **Collecting viruses as viral supernatant:** transferring the supernatant from transfected Φnix cells into a 15 ml falcon tube

5. **Preparing Jurkat Cells:**

    (a) mixing Jurkat cells in their medium by carefully pipetting solution up and down multiple times to break up cell clusters

    (b) counting the cells in Neubauer chamber

    (c) transferring 10^6 Jurkat cells into a 10 ml falcon tube per transfection

    (d) spinning cells down at 400×g

    (e) removing supernatant from Jurkat cells

6. **Transducting Jurkat cells:**

    (a) resuspending cells in 4 ml viral supernatant

    (b) adding 10 µg polybrene to cell solution

    (c) adding 1 ml of cell solution to four wells on a 24 well plate

    (d) closing 24 well plate with parafilm

    (e) centrifuging plate at 2000×g, acceleration/deceleration 5/0 at 37 °C for 90 minutes

    (f) adding 1 ml medium (RPMI, full suppl.) to each well

    (g) incubating for one day at 37 °C, 5% CO_2 and high humidity

    (h) collecting cells from all 4 wells and reseeding them into wells

    (i) adding 666 µl TCM to each well

    (j) adding 1 µl of blasticidin (5 µg/ml) to each well to select for those cells carrying a blasticidin resistance gene on the transfected plasmid

A.3   Transient Transfection

Transiently transfected cells express the transfected gene for a limited period of time. The gene does not integrate into the genome and so is not inherited stably to daughter cells.

1. putting 200 µl medium (opti-MEM, serum free) in an Eppendorf tube

2. vortexing and spinning down of DNA

3. pipetting 2 µg DNA in the center of the opti-MEM-filled Eppendorf tube and vortexing immediately

4. vortexing TurboFect transfection reagent

5. pipetting 10 µl TurboFect in the center of the Eppendorf tube and vortexing immediately

6. incubating for 10 minutes at room temperature

7. dripping the prepared DNA solution on top of the cells (seeded in fresh medium)

A.4   Abbreviations

BSA	bovine serum albumin
FN	fibronectin
GFP	green fluorescent protein
HBSS	Hank's Balanced Salt Solution
HT	HaloTag
HTL	HaloTag ligand
MSD	mean square displacement
PBS	phosphate-buffered saline
PDL	poly-D-lysine
PDMS	polydimethylsiloxane
PEG	polyethylene glycol
PFA	polyformaldehyde
PLL	poly-L-lysine
RGD	amino acid sequence of Arginine, Glycine and Aspartic acid
TEM	transmission electron microscopy
TIRF	total internal reflection
TM	transmembrane

A.5 Materials

accutase	Sigma-Aldrich, Missouri, USA
blasticidin	ThermoFisher scientific, Massachusetts, USA
Bovine serum albumin	Sigma-Aldrich, Missouri, USA
DMEM medium	Life Technologies, California, USA
fetal calf serum	Sigma-Aldrich, Missouri, USA
fibronectin	Sigma-Aldrich, Missouri, USA
Formaldehyde 16% methanol-free	Polyscience, Philadelphia, USA
fugene	Promega, Wisconsin, USA
GFP-TM-Ezrin plasmid	Gift from S. Mayor
GFP-TM-Ezrin* plasmid	Gift from S. Mayor
HBSS	Sigma-Aldrich, Missouri, USA
HeLa cells	Gift from H. Stockinger, Vienna
HTL-GFP	Gift from J. Piehler, U. Osnabrück
Jurkat cells	Gift from H. Stockinger, Vienna
L-Glutamine	Sigma-Aldrich, Missouri, USA
LifeAct-GFP plasmid	Gift from Harald Janoviak, IST Austria
Nexterion Epoxycoated coverslip	Schott, Germany
opti-MEM Reduced Serum	ThermoFisher scientific, Massachusetts, USA
PBS	Sigma-Aldrich, Missouri, USA
penicillin-streptomycin	Sigma-Aldrich, Missouri, USA
pgag-pol plasmid	Gift from H. Stockinger, Vienna
phalloidin-AlexaFluor^{TM}647	ThermoFisher scientific, Massachusetts, USA
PLL-PEG-HTL	Gift from J. Piehler, U. Osnabrück
PLL-PEG-RGD	Gift from J. Piehler, U. Osnabrück
pMD2.G plasmid	Gift from H. Stockinger, Vienna
poly-D-lysin	Sigma-Aldrich, Missouri, USA
RPMI medium	Sigma-Aldrich, Missouri, USA
streptavidin	AppliChem, Germany
Triton X-100	Sigma-Aldrich, Missouri, USA
TurboFect Transfection reagent	Invitrogen, Massachusetts, USA
Utrophin-mEos3.2 plasmid	Gift from H. Janoviak, IST Austria
verapamil	tebu-bio, France

References

[1] J. Bernardino de la Serna, G. J. Schütz, C. Eggeling, and M. Christian. "There Is No Simple Model of the Plasma Membrane Organization". *Frontiers in Cell and Developmental Biology* 4 (2016), p. 106.

[2] A. Kusumi and Y. Sakot. "Cell surface organization by the membrane skeleton". *Current Opinion in Cell Biology* 8 (1996), p. 566.

[3] D. E. Koppler, M. P. Sheetz, and M. Schindler. "Matrix control of protein diffusion in biological membranes". *Proceedings of the National Academy of Sciences* 78 (1981), p. 3576.

[4] A. Kusumi, Y. Sako, and M. Yamamoto. "Confined Lateral Diffusion of Membrane Receptors as Studied by Single Particle Tracking (Nanovid Microscopy). Effects of Calcium-induced Differentiation in Cultured Epithelial Cells". *Biophysical Journal* 65 (1993), p. 2021.

[5] A. Kusumi, C. Nakada, K. Ritchie, K. Murase, K. Suzuki, H. Murakoshi, R. S. Kasai, J. Kondo, and T. Fujiwara. "Paradigm Shift of the Plasma Membrane Concept from the Two-Dimensional Continuum Fluid to the Partitioned Fluid: High-Speed Single-Molecule Tracking of Membrane Molecules". *Annual review of biophysics and biomolecular structure* 34 (2005), p. 351.

[6] S. Löchte, S. Waichman, O. Beutel, C. You, and J. Piehler. "Live cell micropatterning reveals the dynamics of signaling complexes at the plasma membrane". *The Journal of Cell Biology* 207 (2014), p. 407.

[7] B. Alberts, A. Johnson, J. Lewis, M. Raff, K. Roberts, and P. Walter. "Molekularbiologie der Zelle". *Wiley-VCH* (2011).

[8] M. Brameshuber and G. J. Schütz. "Single Molecule Measurements in Membranes". *Comprehensive Biophysics* 5 (2012), p. 337.

[9] T. Fujiwara, K. Ritchie, H. Murakoshi, K. Jacobson, and A. Kusumi. "Phospholipids undergo hop diffusion in compartmentalized cell membrane". *The Journal of Cell Biology* 157 (2002), p. 1071.

[10] Y. Sako and A. Kusumi. "Compartmentalized Structure of the Plasma Membrane for Receptor Movements as Revealed by a Nanometer-level Motion Analysis". *The Journal of Cell Biology* 125 (1994), p. 1251.

[11] K. Gowrishankar, S. Ghosh, S. Saha, R. C., S. Mayor, and M. Rao. "Active Remodeling of Cortical Actin Regulates Spatiotemporal Organization of Cell Surface Molecules". *Cell* 149 (2012), p. 1353.

[12] P. Singh, C. Carraher, and J. Schwarzbauer. "Assembly of Fibronectin Extracellular Matrix". *Annual Review of Cell and Developmental Biology* 26 (2010), p. 397.

[13] URL: `https://www.thermofisher.com/at/en/home/life-science/cell-analysis/labeling-chemistry/fluorescence-spectraviewer.html`.

[14] URL: `http://olympusmicro.com/primer/java/jablonski/jabintro/index.html`.

[15] M. Melak, M. Plessner, and R. Grosse. "Actin visualization at a glance". *Journal of Cell Science* 130 (2017), p. 525.

[16] A. M. Arnold. "Probing the Plasma Membrane Organisation at the Nanoscale". MA thesis. Johannes Kepler Universität Linz, 2015.

[17] B. J. Berlin, L. M. Goins, and D. R. Mullin. "Comparative analysis of tools for live cell imaging of actin network architecture". *BioArchitecture* 4 (2015), p. 190.

[18] L. N. Munsie, N. Caron, C. R. Desmond, and R. Truant. "Lifeact cannot visualize some forms of stress-induced twisted f-actin". *Nature Methods* 6 (2009), p. 317.

[19] A. Smoligovets, A. Smith, and J. Groves. "Ratiometric Imaging of the T-Cell Actin Cytoskeleton Reveals the Nature of Receptor-Induced Cytoskeletal Enrichment". *Biophysical Journal* 105 (2013), p. L11.

[20] URL: `http://www.grid-tech.com/catalog.htm`.

Acknowledgments

I would like to thank Gerhard Schütz. After listening to his first lecture, I knew that I wanted to do my master's thesis in his group. He was always able to broaden my horizon and increase my interest with inspiring remarks and questions.

My supervisor Eva Sevcsik introduced me, with all patience and care one could hope for, to the new topic of molecular biology and biochemistry. Throughout this work she supported me and increased my capabilities and was always open for discussion and questions. She is an inspiration to me, not only in the professional world.

But all this would not have been possible without the extraordinary support from my parents Sonja and Walter Koffler! Ihre Freude über meinen Abschluss hat mir erst bewusst gemacht was ich geschafft habe. Sie haben immer mit großem Interesse verfolgt welche Wege ich gehe und haben mich auf all diesen unterstützt. Auch wenn sie stolz sind auf meine Leistungen haben sie mir immer gezeigt dass meine Freude und mein Glück ihnen noch mehr am Herzen liegen. Ich danke euch für eure Liebe und eure Freude, ich bin dankbar eure Tochter zu sein!

Last but not least I would like to mention two important fellow students of mine who were with me from the start of my studies. It was due to Iris Schmidt's organizational talent that I did not mess up my first semesters, and her time management has given me the needed boost to finish writing this thesis. It was always fun to mess around with her and explore extra-curricular activities! David Toneian has grown to be an important part of my life. He is always there for me and manages to decrease my stress level before exams to a bearable amount. Thank you so much for proofreading this thesis multiple times and for all your input and support!